EARTH SURFACE PROCESSES AND LANDFORMS
Earth Surf. Process. Landforms **34**, 848–859 (2009)

Published online 13 February 2009 in Wiley InterScience
(www.interscience.wiley.com) DOI: 10.1002/esp.1779

Spatial variability of rainfall on a sub-kilometre scale

P. Fiener[1]* and K. Auerswald[2]
[1] Department of Geography, Hydrogeography and Climatology Research Group, Universität zu Köln, Cologne, Germany
[2] Lehrstuhl für Grünlandlehre, Technische Universität München, Freising-Weihenstephan, Germany

Received 6 March 2008; Revised 31 October 2008; Accepted 12 November 2008

* Correspondence to: P. Fiener, Department of Geography, Hydrogeography and Climatology Research Group, Universität zu Köln, Albertus Magnus Platz, D-50923 Cologne, Germany. E-mail: peter.fiener@uni-koeln.de

ESPL
Earth Surface Processes and Landforms

ABSTRACT: The variability of rainfall in space and time is an essential driver of many processes in nature but little is known about its extent on the sub-kilometre scale, despite many agricultural and environmental experiments on this scale. A network of 13 tipping-bucket rain gauges was operated on a 1·4 km^2 test site in southern Germany for four years to quantify spatial trends in rainfall depth, intensity, erosivity, and predicted runoff. The random measuring error ranged from 10% to 0·1% in case of 1 mm and 100 mm rainfall, respectively. The wind effects could be well described by the mean slope of the horizon at the stations. Except for one station, which was excluded from further analysis, the relative differences due to wind were in maximum ±5%. Gradients in rainfall depth representing the 1-km^2 scale derived by linear regressions were much larger and ranged from 1·0 to 15·7 mm km^{-1} with a mean of 4·2 mm km^{-1} (median 3·3 mm km^{-1}). They mainly developed during short bursts of rain and thus gradients were even larger for rain intensities and caused a variation in rain erosivity of up to 255% for an individual event. The trends did not have a single primary direction and thus level out on the long term, but for short-time periods or for single events the assumption of spatially uniform rainfall is invalid on the sub-kilometre scale. The strength of the spatial trend increased with rain intensity. This has important implications for any hydrological or geomorphologic process sensitive to maximum rain intensities, especially when focusing on large, rare events. These sub-kilometre scale differences are hence highly relevant for environmental processes acting on short-time scales like flooding or erosion. They should be considered during establishing, validating and application of any event-based runoff or erosion model. Copyright © 2009 John Wiley & Sons, Ltd.

KEYWORDS: rainfall variability; rain intensity variability; runoff; rainfall measurement

Introduction

The variability of rainfall in space and time is an essential driver of many processes in nature. This is most obvious for questions such as the analysis and modelling of rainfall–runoff relations (e.g. Bronstert and Bárdossy, 2003; Faurès *et al*., 1995; Kirkby *et al*., 2005) or soil erosion processes (e.g. Nyssen *et al*., 2005; Nearing, 1998), but it is also important for characteristics such as spatial-temporal variability of crop yields, patterns of deposits from atmosphere, soil carbon and nitrogen turnover, etc.

Spatial variability of rainfall on a scale >100 km^2 has been an important topic in hydrology and meteorology research during the last decades. Studies focused on methods to improve the interpolation of rain gauge point measurements (e.g. Syed *et al*., 2003; Borga and Vizzaccaro, 1997; Kruizinga and Yperlaan, 1978), optimizing rain gauge networks (e.g. Papamichail and Metaxa, 1996; Bastin *et al*., 1984), or utilizing remote sensing data, especially ground-based radar measurements (e.g. Borga, 2002; Datta *et al*., 2003; Quirmbach and Schultz, 2002; Tsanis *et al*., 2002; Berne *et al*., 2004), to determine the spatial variability of rainfall. On smaller scales (10–100 km^2) studies are rarer and test sites are mostly located in areas where strong gradients in rainfall can be expected due to orographic effects in mountainous regions (e.g. Buytaert *et al*., 2006; Arora *et al*., 2006) or at coast lines (e.g. Stow and Dirks, 1998), or due to climatic situations with distinct convective storms (e.g. Desa and Niemczynowicz, 1997; Hernandez *et al*., 2000; Berne *et al*., 2004).

On a smaller scale (<10 km^2), where many environmental processes are often studied in detail and where rainfall–runoff or erosion models are mostly developed and tested only sparse knowledge exists on the variability of rainfall depth and intensity (e.g. Goodrich *et al*., 1995; Jensen and Pedersen, 2005; Taupin, 1997; Sivakumar and Hatfield, 1990). Information is needed about the extent and significance of rain variability on this scale, for example to develop and validate erosion and rainfall–runoff models (e.g. Faurès *et al*., 1995; Johannes, 2001), to understand small-scale variability in soil moisture and hence soil properties, to design urban water management facilities (e.g. Berne *et al*., 2004), or to validate subscale variability in rain radar data (e.g. Jensen and Pedersen, 2005).

The overall aim of this study was to determine the spatial variability in rainfall depth and maximum intensity, as well as

variability of derived parameters within a small test site (1·4 km^2) with 13 measuring stations. More specifically the objectives were to:

(i) Determine the importance of spatially variable events during the four-year observation period.
(ii) Analyse the extent of spatial variability for the total rain depth and the maximum intensities on an event basis.
(iii) Analyse the resulting spatial variability of parameters non-linearly related to rainfall, exemplarily shown for rainfall erosivity and predicted daily runoff.

Material and Methods

Test site

Precipitation was measured at the Scheyern Experimental Farm (Figure 1), which is located about 40 km north of Munich (48°30′50″ N, 11°26′30″ E). The orography, soils and land use of the area are typical for the Tertiary Hills, an important extensively used agricultural landscape in central Europe. The rolling topography of the test site covered an area of approximately 1·4 km^2 of arable land at an altitude of 446 to 500 m above mean sea level (Sinowski and Auerswald, 1999). The mean annual air temperature, measured at the central meteorological station within the experimental farm, was 8·4 °C (for 1994–1998). The measured precipitation was 789 mm yr^{-1} (for 1994–1998) with the highest values occurring from May to August and the lowest occurring in the winter months.

Measurements

Precipitation was measured between April 1994 and March 1998 at 13 locations within the 1·4 km² research site (Figure 1). To measure precipitation continuously during the winter months eight of the rain gauges were heated. For this study, focusing on rain, we used only measurements from the hydrological summer half-year (May–October) when all stations were operational. Measurements were carried out 1·0 m above the ground using automated 0·02–0·04 m^2 tipping bucket rain gauges (Table I). Stations A01–A10 measured precipitation only, while at the stations B01–B03 wind speed, air and soil temperatures at different levels and several other meteorological data were measured as well. The tipping-bucket rainfall data from all stations were aggregated to minute values.

For the analysis of spatial trends of precipitation the characteristics of single events were compared. Therefore, rain events (subsequently referred to as events) were defined as rainfall periods separated from preceding and succeeding rainfall by at least 6 h, during which uncorrected rain larger than 5 mm

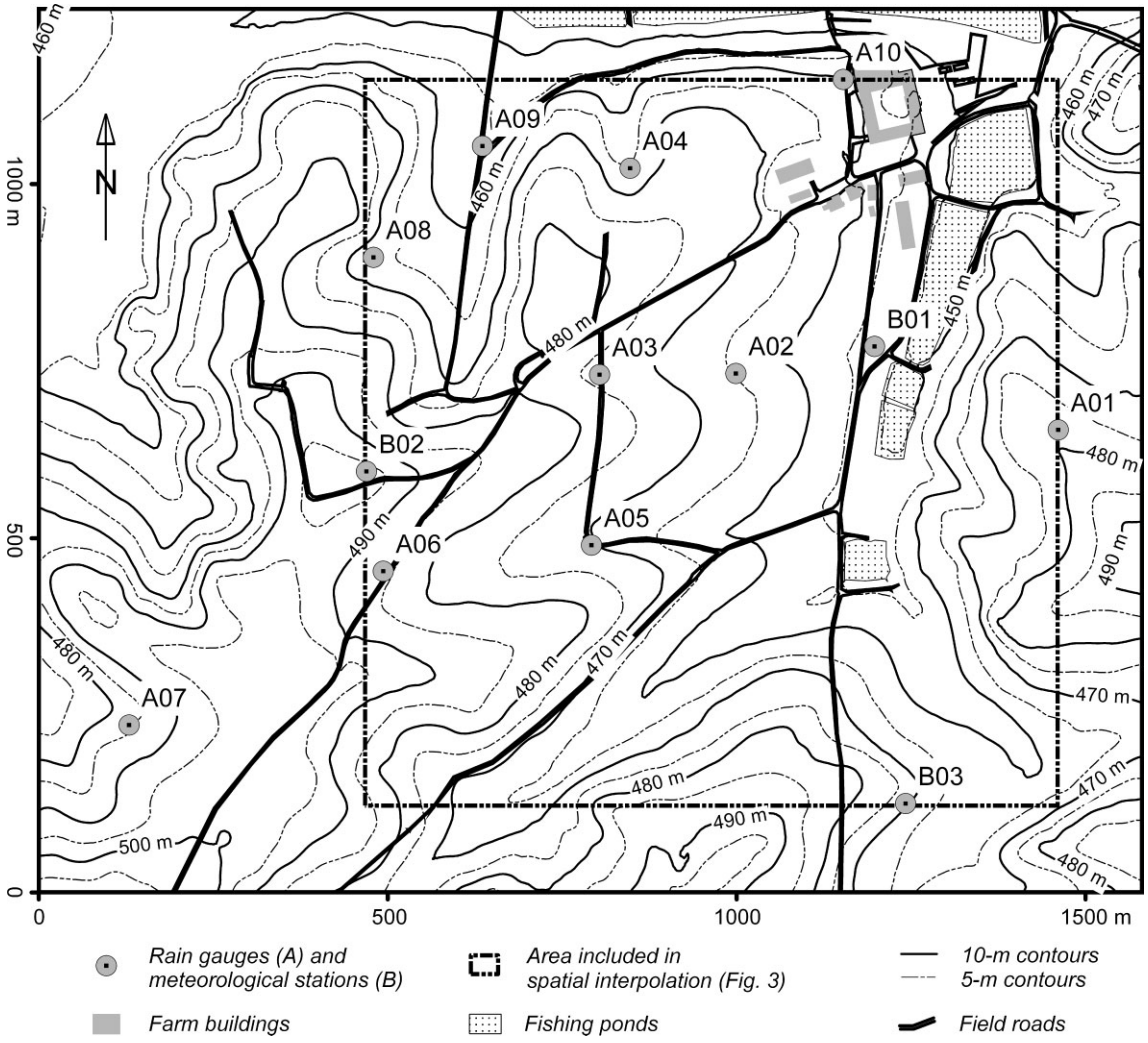

Figure 1. Topography of the test site in the Scheyern (southern Germany) including location of all rain gauges (A01–A10) and meteorological stations (B01–B03).

DOI: 10.1002/esp

Table I. Altitude, mean slope of the horizon and technical data of the measuring stations

Station	Altitude a.s.l. (m)	Slope of the horizon[a] (deg)	Measuring resolution (mm)	Collecting area (m²)	Manufacturer
B01	453	4·8	0·2	0·04	Casella, UK
B02	496	3·0	0·2	0·04	Casella, UK
B03	471	10·9	0·1	0·04	Casella, UK
A01	477	0·5	0·1	0·02	Seba, Germany
A02	465	3·8	0·1	0·02	Seba, Germany
A03	475	7·6	0·1	0·02	Seba, Germany
A04	466	4·5	0·1	0·02	Seba, Germany
A05	470	8·0	0·1	0·02	Seba, Germany
A06	486	8·4	0·1	0·02	Seba, Germany
A07	485	6·9	0·1	0·02	Seba, Germany
A08	468	8·9	0·1	0·02	Seba, Germany
A09	456	5·6	0·1	0·02	Seba, Germany
A10	460	7·3	0·1	0·02	Seba, Germany

[a] Calculated assuming harvested fields using an approach developed by Richter (1995) from measurements in 15° segments, which were weighted according to the mean distribution of wind directions.

was measured at Station B01, B02 or 50% of all stations, this is analogous to the definition of an erosive event by Wischmeier and Smith (1978).

To identify erroneous measurements and to prevent persistent failure of single stations, e.g. due to insects, leaves, etc. trapped in the collecting funnel of the tipping buckets, observed rain depths and characteristics were controlled monthly. Moreover, the event durations at the different stations were compared to identify stations with prolonged rain events often indicating a plugged collecting funnel. In the case of any suspicious findings in the data the equipment of the identified station was checked and the measurements were rejected if necessary.

As known from a number of studies the accuracy of tipping bucket rain gauges is sensitive to rain intensity, which was compensated either by correction functions (e.g. Adami and Da Deppo, 1986; Molini *et al*., 2005; La Barbera *et al*., 2002) or by improving measuring techniques (e.g. Overgaard *et al*., 1998). For this study three of the tipping bucket rain gauges were tested under different rain intensities in the laboratory to derive intensity dependent correction functions. For rain intensities <30 mm h^{-1}, which represent more than 90% of all measured rain events at the test site, no significant relationship between rain intensity and measuring error could be found. However, larger tendencies than those measured in the laboratory experiments can be expected due to a slight fouling of equipment installed for field measurements. The tipping bucket error of the field measurements was determined by collecting the rain water intercepted by the gauges in small tanks buried below ground level near the measuring device. These small tanks were emptied bi-weekly to determine total rain depth which was used to correct the tipping bucket data. Both measurements were closely correlated at all 13 stations ($R^2 > 0{\cdot}998$), nevertheless a deviation of the tipping bucket measurements between –7% to +8% was found (mean absolute deviation being 3%). The station-dependent relation was used to adjust the tipping bucket data with individual correction factors ranging between 0·927 (A06) and 1·081 (B03).

Quantifying spatial variability due to wind effects

Using rain gauges at a height of 1 m above ground causes wind effects which result in differences between measured rain and actual rain reaching the surface. These differences were investigated with additional surface-level rain gauges at the meteorological stations B01 and B02 (Johannes, 2001). For this study dealing with the spatial distribution of rain depth and intensity it is important to focus on differences in wind effects between the 13 rain stations. Such differences can be expected due to different measuring devices and different wind effects mainly caused by different slopes of the horizon at the measuring locations (Table I). To detect wind effects we firstly categorized all events in: (i) events with spatially random variability in rainfall distribution and (ii) events with spatially systematic variability in rainfall distribution (see next sub-section).

The rainfall of events with spatially random variability was accumulated for each station and a regression analysis was carried out using this accumulated rainfall and the mean slope of the horizon of the individual station. For all A-stations, except A07, and station B03 the difference in rainfall correlated with $R^2 = 0{\cdot}63$ (probability that R is different from zero, $p = 0{\cdot}01$) with the difference in topographic sheltering (Figure 2), which is used here as a proxy for wind effects.

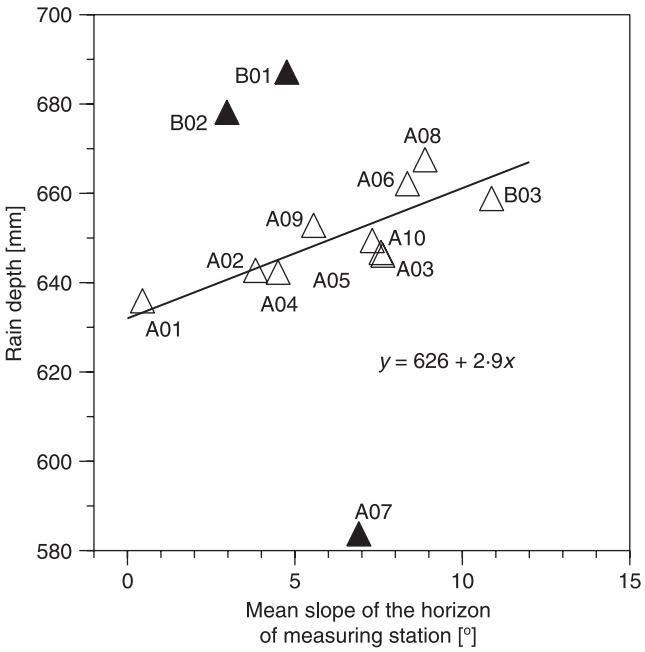

Figure 2. Mean slope of the horizon of the measuring stations versus rain depth of all random events during the hydrological summer-half years (1994–1997); regression line calculated for all A-stations (except A07) and station B03 represented by unfilled triangles ($R^2 = 0{\cdot}63$, $n = 9$).

DOI: 10.1002/esp

The rain depth at the individual A-stations deviated by not more than 2% from the average of all A-stations (excluding A07) if total rain of all random events was accumulated. At A07, however, the rainfall of all random events was 11% smaller on average compared to all other A-stations. This significant difference (two-sided *t*-test; null hypothesis mean of all A-stations equal to mean of station A07) was probably caused by higher wind speeds due to the location of A07 in a small depression canalizing wind coming from south and south-west, which are the dominant wind directions of the area (representing 59·2% of all wind directions). At stations B01 and B02 the measured rain decreased less with increasing wind speed than at the A-stations (inclusive B03). In total 5% more rain than the average of all A-stations (except A07, inclusive B03) was measured for all events during the hydrological summer-half year. The major reason probably was the aerodynamically more appropriate design of the B01 and B02 rain gauges with a slightly different slope of the rim of these two stations (Johannes, 2001).

When analysing the wind effects at the stations B01 and B02, where additional surface-level rain gauges were installed, we found a larger measuring error at B02 for accumulated rainfall (1994–1998) of 7% compared to 5% at station B01. This difference can be attributed to higher average wind speeds of 2·3 m s^{-1} at B02 compared to those of 1·3 m s^{-1} at B01. Nevertheless, the analysis of single rain events did not allow a clear relationship to be derived between wind speed and measuring error for each of the stations, because the size of the errors also depended strongly on rain characteristics. In general, the relative error decreased with increasing event size, for example all events <10 mm had a relative error of 9·0%, while this decreased to 4·2% for all larger events.

The average wind speed during all events with spatially systematic variability [1·7 m s^{-1}, standard deviation (SD) = 0·3 m s^{-1}] was significantly lower compared to the spatially random events (2·4 m s^{-1}, SD = 1·3 m s^{-1}) (two-tailed *t*-test, null hypothesis is equality of means). Hence, as we focus on rainfall events with a spatially systematic variability, no corrections for wind speed were applied due to the total relatively small random error caused by wind effects in the case of these events and the general difficulties to derive clear correction functions. Only measurements from station A07 were excluded from further evaluations due to its specific sensitivity to wind speed. If we use or refer to average rain depths these are calculated according to the Thiessen polygon areas varying between 4·7 and 18·5 ha for the individual stations (excluding A07) within the rectangle stretched by the measuring locations shown in Figure 1.

Defining spatially random and spatially systematic variability in rainfall distribution

To distinguish between events, where the spatial variation of rain was random due to measuring errors and those events with a spatially systematic variability, a multiple regression analysis was performed, applying a linear, an exponential or a polynomial function. For these regression models, using rain depth regressed on *X*–*Y*-coordinates of the stations, the null hypothesis that the coefficients of the model (except for intercept) were different from zero was tested applying *t*-statistics. Events are defined as events with a spatially systematic variability in rainfall distribution (subsequently referred to as gradient events) if one of the model coefficients or the total regression model is highly significant ($p < 0{\cdot}01$). If the null hypothesis holds not true on this significance level the events were categorized as events with a spatially random variability in rainfall distribution (subsequently referred to as random events). The residuals of the gradient events were then tested for normal distribution and autocorrelation (see later) to examine whether the regression model was appropriate to describe the spatial trend.

To illustrate and discuss the spatial variability of rainfall events within the research area without a predefined spatial model, geostatistical analyses [for theory see Webster and Oliver (2000) and Nielsen and Wendroth (2003)] were carried out for four exemplary gradient events. Semivariograms were constructed with the supplementary package geoR (Diggle and Ribeiro Jr, 2007) of the statistical software GNU R, version 2·6 (R Development Core Team, 2007). For semivariance analysis rain gauge readings of all four gradient events were pooled (Voltz and Webster, 1990) to meet the requirement of at least 30–50 data sets ($n = 48$). According to Schuurmans *et al*. (2007) a pooled semivariogram is almost as good as using event-based semivariograms. Prior to pooling, the data of the individual rains were scaled to a mean of zero and a standard deviation of one to attain second order stationarity among rains. This resulted in an empirical semivariogram, which closely followed a Gaussian model (nugget 0·06, sill 5·09, range 1333 m, Nash–Sutcliffe index 0·9356) where 12 lag classes were weighted according to *n*/lag when fitting the semivariogram model to give more weight to those lag classes, which contained many data pairs and which were closer to the origin and thus more important for kriging. The small nugget effect and the large sill indicated a strong pattern of the rains compared to the uncertainty. This semivariogram model and the scaled data of the individual rains were then used to construct rain maps by block kriging using 10×10 m^2 blocks with the package gstat (Pebesma, 2004), which were finally rescaled to millimetre units with the mean and standard deviation of the individual rains.

Analysis of the regressions, analysis of the residuals and the exemplarily geostatistically interpolated rain maps (Figure 3), all indicated that the resulting gradient events generally followed a more or less linear trend. Hence, rain depth was then linearly regressed on the *X*–*Y*-coordinates of the stations to determine the mean trend for each gradient event, which later on is used for an easy comparison and further analysis of the resulting trends. Analogously to the spatial interpolation of the four exemplary gradient events a semivariogram was calculated by pooling all gradient events prior and after correcting for the trend by regression analysis to examine to which degree the linear regression equations with predefined spatial behaviour adequately quantified and removed the spatial trend and how much autocorrelation was left in the residuals of the regression analysis.

Parameters derived from rainfall – rain erosivity and runoff prediction

To elucidate the effects of spatial gradient events on environmental processes at the sub-kilometre scale it is necessary to focus on driving parameters derived form rainfall depth, which may translate rainfall variability sub- or super-proportional to the respective process. As an example for such a parameter the rain erosivity was calculated, which is commonly used to describe the rain potential to detach soil particles and to initiate soil erosion caused by surface runoff. Rain erosivity originally was introduced with the Universal Soil Loss Equation (USLE; Wischmeier and Smith, 1960) and now it is used in many soil erosion models. Rain erosivity R_e is calculated according to Equation 1 for all erosive events, defined as events with at least 10 mm of precipitation or a maximum intensity above 10 mm h^{-1} (Schwertmann *et al.*, 1987).

DOI: 10.1002/esp

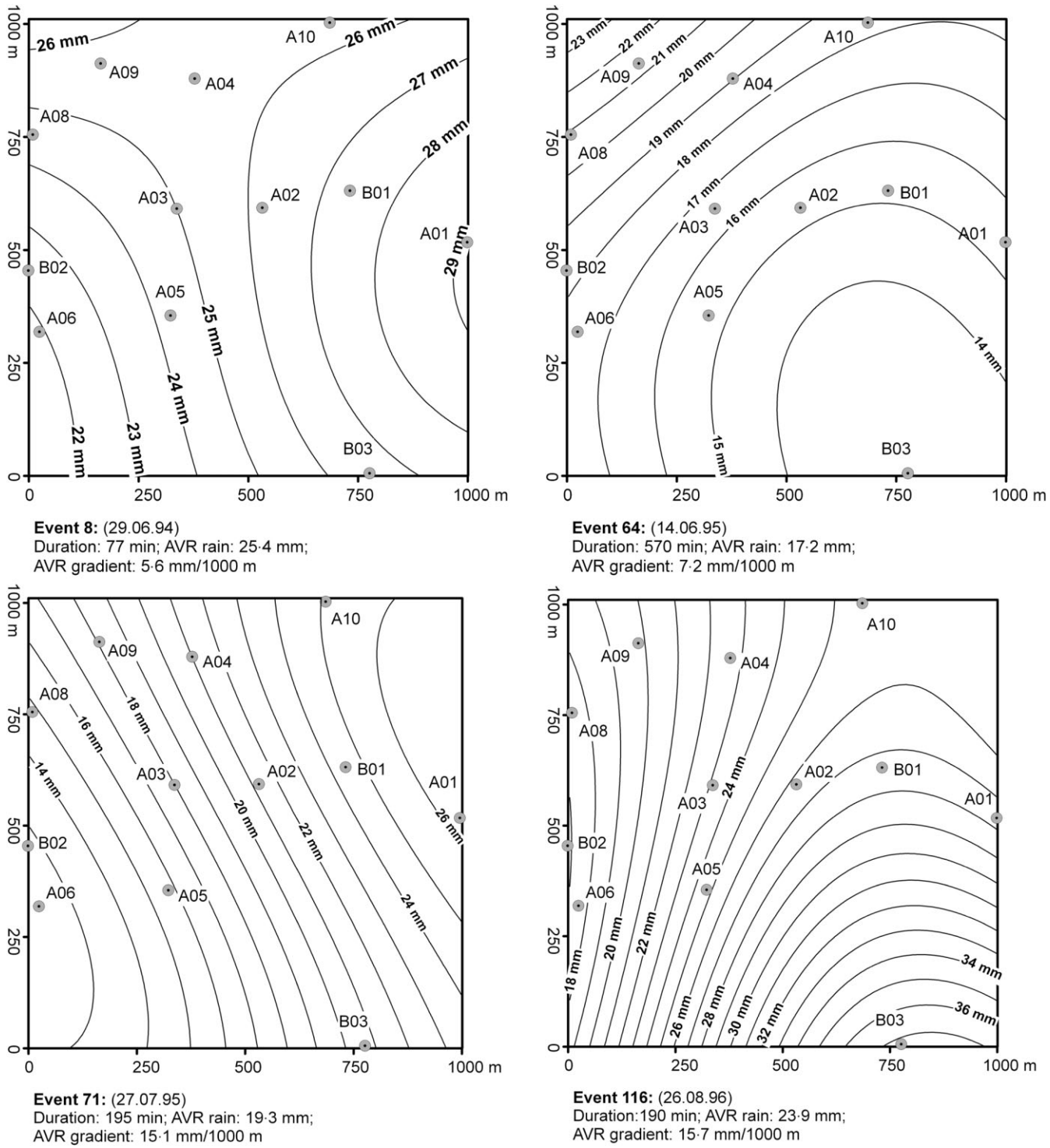

Figure 3. Interpolation of rain depth (in mm) of four gradient events by block kriging for 10×10-m^2 blocks; the twelve locations of the measuring stations (A01–A06, A08–A10, B01–B03) are indicated by grey circles; for each four events its duration, average rain depth (AVR rain) calculated from the geostatistical interpolation and average gradients in rain depth (AVR gradient) are given. Krige standard deviations averaged over all 10×10-m^2 blocks are 0·4, 0·5, 0·9 and 1·1 mm for rains 8, 64, 71 and 116, respectively.

$$R_e = E \times I_{max30} \quad (1)$$

$$E = \sum_{i=1}^{n} E_i \quad (2)$$

with:

$E_i = ((11{\cdot}89 + (8{\cdot}73 \log I_i))\, N_i\, 10^{-3}$ for $0{\cdot}05 \le I_i \le 76{\cdot}2$

$E_i = 0$ for $I_i < 0{\cdot}05$

$E_i = 28{\cdot}33\, N_i 10^{-3}$ for $I_i > 76{\cdot}2$

where E is the total kinetic energy of an event (in kJ m^{-2}), I_{max30} is the maximum 30-min rain intensity of an event (in mm h^{-1}), i is a time interval during the event with a constant rain intensity, E_i, I_i, and N_i are kinetic energy, rain intensity and accumulation within time interval i, respectively.

In addition daily runoff was calculated for the days with gradient rains applying the Soil Conservation Service (SCS) curve number model (Mockus, 1972). Two contrasting situations on Hydrological Soil Group C were assumed, either small grain favouring infiltration (curve number 81) or row crops more likely favouring runoff (curve number 85)

DOI: 10.1002/esp

which both corresponded to the land use on the experimental farm (Fiener and Auerswald, 2007).

Results

In total 115 events ≥ 5·0 mm were observed in the four hydrological summer-half years (1994–1997). These events were measured at least at eight of the 13 measuring stations (including A07). In case of 52 events all 13 stations were operating. On average between 2·5 (October) and 6·8 events (August) per month occurred during the observation period. These events represent 67% (September) to 90% (July) of the total rain amount in these months. The largest rainfall was 62·2 mm, while the mean and the median of all events in the hydrological summer-half years were 12·6 mm and 9·3 mm, respectively.

When applying the multiple regressions to determine gradient events, the linear, exponential and polynomial models showed similar levels of significance and similar R^2 values. The curvilinear regression surfaces were with few exceptions not significantly [tested according to Samiuddin (1970)] better than the linear model. This justified using a linear trend for further analysis in addition to the definition of scale associated with the linear model. Also the geostatistical interpolation examples (Figure 3) justified the use of a linear trend. For 38 events during the hydrological summer-half year the linear regression was at least highly significant ($p < 0{\cdot}01$). The R^2 for the linear regressions ranged between 0·59 and 0·96, with 50% of all $R^2 > 0{\cdot}81$. Geostatistical analysis of the pooled residuals showed that the linear regressions had eliminated 92% of the pattern as the partial sill dropped from 2·7 to 0·21 with Gaussian models in both cases. The partial sill was less than half as large as the nugget effect for the residuals. The analysis of the model residuals individually for each event, as an example shown for events 8 and 64 (Figure 4), indicated that in case of 34 events (e.g. event 8) the model assumptions (normal distribution and no autocorrelation of residuals) are reasonably met. For four events (including event 64) this was less clear as size of residuals show some spatial clustering and/or residuals are not normal distributed indicating that the trend may be curvilinear but this would not change any conclusion drawn from the simplification of a linear trend within the restricted research area. Hence, we also categorized these events as gradient events. The (almost) linear trends indicate that the precipitation cells causing the trend were larger than the research area and had their minimum and/or maximum outside the research area.

The events were categorized in four sections (0–90°, 90–180°, 180–270° and 270–360°) to determine if the gradients had a preferred direction. The null hypothesis that the number of observed events per section is not significantly different from the equal distribution could not be rejected on a 5% level applying a Pearson Chi-square test (alternative hypothesis: observations are different from an equal distribution). This corresponds with the notion of precipitation cells of random position relative to the research site.

During the hydrological summer-half year the gradient events only occurred between May and September (Figure 5)

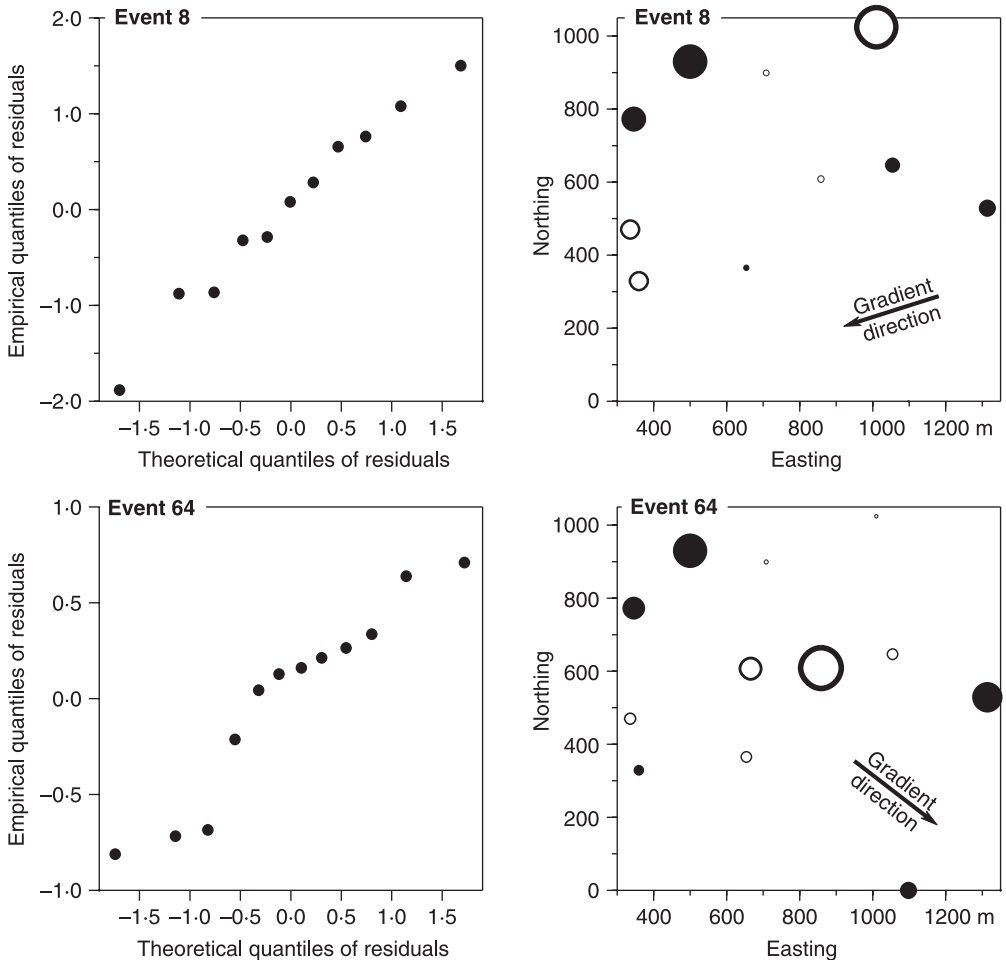

Figure 4. Analysis of normal distribution (left panels) and spatial distribution (right panels) of residuals derived from linear regression models ($p < 0{\cdot}001$) for two gradient events ($R^2 = 0{\cdot}78$ and 0·91 for top and bottom); positive residuals are displayed by black markers, negative residuals by white markers; marker size indicates the value; event 8 exhibited a random distribution of the residuals while event 64 seemed to have a curvilinear trend; the arrows indicate the direction of the gradients, which were 5·6 and 7·2 mm km^{-1} for event 8 and 64, respectively.

DOI: 10.1002/esp

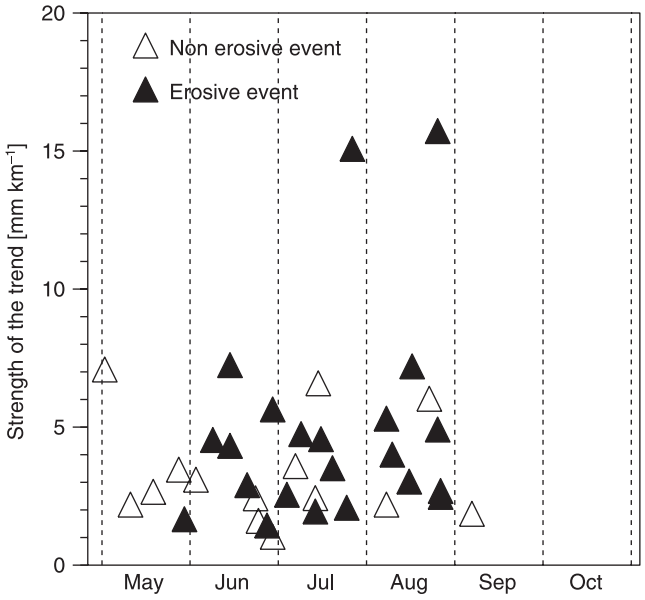

Figure 5. Date and strength of gradient events in the hydrological summer-half-years from 1994 to 1997.

Table II. Statistical data of all 38 rain events with a trend in rain depth observed in the hydrological summer-half-years 1994–1997; rain gradient was calculated with multiple linear regressions using station coordinates (northing and easting); the relative rain gradient was derived from the rain depth at the spatial centre of the test site, which was defined as the average of the station coordinates of B01 and B02; rain depth for the centre point was also calculated with the regression functions

	Rain amount (mm)	Rain gradient (mm km^{-1})	Relative rain gradient (% km^{-1})
Mean	12·1	4·2	48
Median	9·9	3·3	36
1st quartile	6·1	2·2	20
3rd quartile	17·2	5·1	47
Minimum	2·4	1·0	9
Maximum	28·9	15·7	278

with a median rain gradient of 3·3 mm km^{-1} (Table II). In case of four relatively small events close to our threshold of $N > 5{\cdot}0$ mm the gradient was greater than the average rainfall. For 95% of all gradient events the rain gradient was < 7·5 mm km^{-1}, while in two cases, which occurred in July and August, a gradient > 10 mm km^{-1} was measured. Except for these two events the frequency of events with high or low rain gradients was similar between June and August (Figure 5).

Sixteen out of 38 gradient events did not meet the definition of erosive rain events. These non-erosive gradient events had a median rain depth of 5·9 mm and a median rain gradient of 2·7 mm km^{-1}, thus both were smaller than for the erosive gradient events (median rain depth 15·1 mm, median rain gradient 4·2 mm km^{-1}). Within both groups the gradient did not depend on rain depth.

Within the hydrological summer-half years (1994–1997) 59 erosive events were identified out of which 22 (37%) were erosive trend events. A trend is hence not unlikely for erosive rains. Most erosive gradient events occurred between June and August (Figure 5). As these months contribute about 70% to annual erosivity in this region (Schwertmann *et al.*, 1987) and the erosive events are highly relevant for the simulation of runoff and soil erosion under agricultural land we subsequently focus on the months June to August.

Between June and August 42 erosive events, representing 70% of the total precipitation of 1124 mm, were recorded (1994–1997) (Table III). The number and the amount of rain of these events were more or less equally distributed within all months. Approximately half of the events had a spatial trend. Hence, on the temporal scale of events the general assumption of a spatially homogeneous rain input used in many small-scale runoff and erosion models is not justified. While the spatially random events produced about 20% more rain than gradient events, the cumulative rain erosivity of the gradient events was about 40% larger. Variation in rain erosivity was up to 255% and thus much more pronounced than the variation in total rain depth (maxima < 100% for rains > 6 mm). This super-proportional effect on rain erosivity was caused by differences in rain intensity. While the rain depth differed within the area during a gradient event, the duration of the rain remained greatly unchanged. An increasing rain depth, hence, also increased intensity because rain duration remained unchanged. Thus, in the calculation of the rain erosivity (Equation 1) the maximal 30-min intensity (I_{max30}) and the total kinetic energy changed and thus led to the super-proportional effect. The median as well as the 1st and 3rd quartile of I_{max30} for all gradient events was about 1·5 times larger than for all spatially random events. For predicted runoff the effect was even larger, because most of the rainfall would infiltrate under the assumed conditions leading to steep gradients of the excess rainfall. The predicted gradients relative to the spatial average were about two to 20 times larger for runoff than for rain depths (Figure 6).

For the effects of gradient events, e.g. on erosion, runoff accumulation and peak discharge, the spatio-temporal variability of rainfall also becomes relevant. As an example this was analysed for the four events with the largest trends (event numbers 8, 64, 71, and 116) for which the spatial distribution is shown in Figure 3. Within its first 60 min

Table III. Total rain depth, total erosive rain depth and rain erosivity, R_e, for the summer months June, July and August (1994–1997)

		June	July	August	Sum
Total rain depth (mm)		336	396	391	1124 (1130)[a]
Proportion of erosive events (%)		66	76	66	70
Number of erosive events	Without trend	6	8	7	21
	With trend	6	7	8	21
Rain depth of erosive events (mm)	Without trend	133	189	108	430
	With trend	88	113	151	352
ΣR_e (N h^{-1})	Without trend	12	48	27	87
	With trend	47	23	53	123

[a] Average rain depth (1961–1990) measured at the German Weather Service (DWD) station in Scheyern located about 1 km east of the test site.

DOI: 10.1002/esp

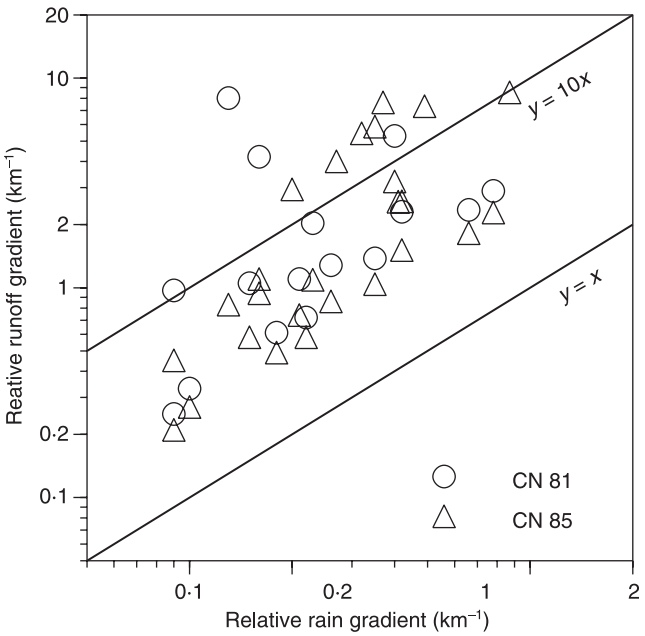

Figure 6. Gradients in rain and runoff depths (excluding rains, for which no runoff was predicted); gradients given in millimetres per kilometre relative to the mean rain and runoff depth in millimetres.

event 8 was the most intense summer storm during the observation period. The difference in precipitation between A06 (22 mm) and A01 (29·1 mm) resulted from only 15 min of different rain intensity (Figure 7). In the eastern part of the test site (A01) rain intensity was nearly constant, while in the western part (A06) intensity decreased during the second half of the event. A similar situation occurred during events 64, 71 and 116 (Figure 7). The differences in total rain depth mainly resulted from short-lasting (<30 min) differences in rain intensity while the difference in rainfall intensity was negligible during most of the rain. This indicates that the stations operated correctly and that the differences in rainfall depths are not caused by systematic errors in the measuring systems.

In most cases trends were caused by short, high intensity bursts and not by different rain duration. Hence, the importance of trends increases with decreasing length of the considered periods (Table IV). Within the 5 min of highest intensity, the median intensity gradient was 24 mm h^{-1} km^{-1} and the maximum gradient even amounted to 49 mm h^{-1} km^{-1}. In contrast, the median gradient in rain depth decreased only from 4·2 to 2·0 mm km^{-1} when the reference period decreased from total rain to 5 min. Hence half of the total gradient evolved during 5 min of rain.

For event 8 (29 June 1994) Figure 8 exhibits large negative and positive differences of intensity in sequence. This behaviour characterizes events during which the high-intensity cell moves over the area and hits a large part of the total area but at different times. The gradient in accumulation was thus partly levelled out already during the event. In most cases, however, (three out of four in Figure 8) these high-intensity cells were quite stationary and thus produced a spatial trend, which was still detectable even for the total rain.

Discussion

High-intensity cells cause the spatial trend on the sub-kilometre scale

Although there was no synoptic analysis of these events, a connection between convective storms typical for these summer months and gradient events is evident. The findings of (i) a nearly linear trend, (ii) a random orientation of the trend,

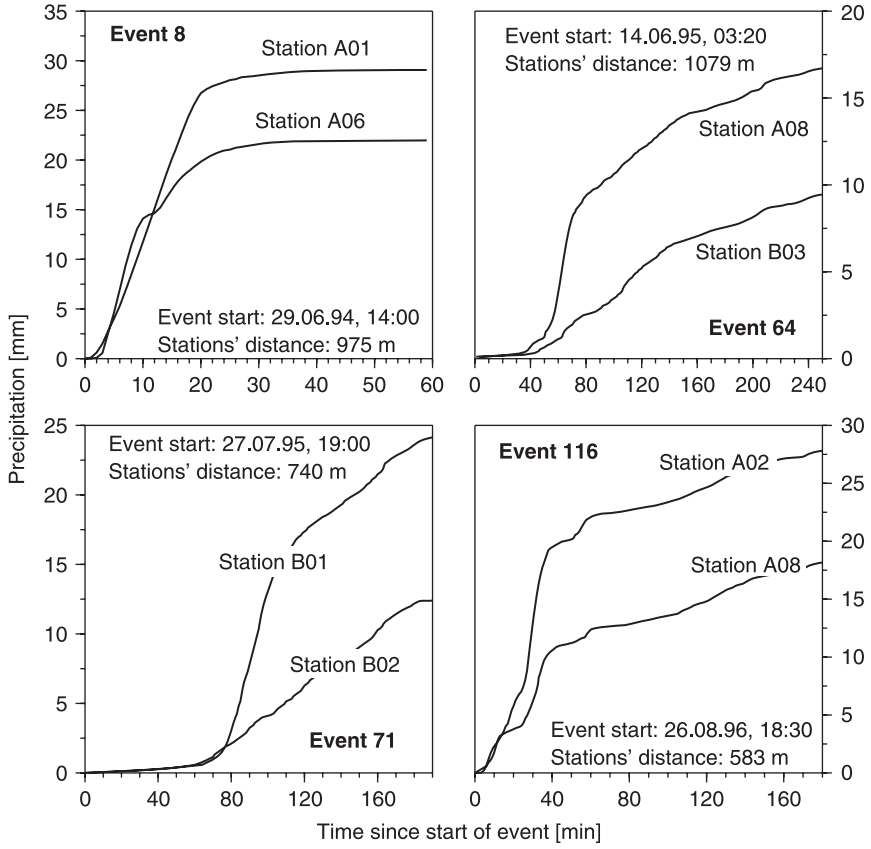

Figure 7. Cumulative rain of the two measuring stations between which the largest trend of rain depth was determined for the four events shown in Figure 3.

DOI: 10.1002/esp

Table IV. Gradients of maximum rain depth and maximum rain intensity for time intervals between 5 and 60 min and gradients of total rain erosivity (in N h^{-1} km^{-1}) for all erosive gradient events (n = 21) in the hydrological summer half-years 1994 to 1997

Rain property	Interval	Median	1st quartile	3rd quartile	Minimum	Maximum
Rain depth gradient (mm km^{-1})	5 min	2·0	1·6	3·6	0·6	4·1
	10 min	2·9	2·2	4·8	0·9	6·0
	15 min	3·3	1·8	4·7	1·0	8·1
	30 min	3·9	1·5	5·4	0·4	13·3
	Total	4·2	2·5	5·3	1·4	15·7
Intensity gradient (mm h^{-1} km^{-1})	5 min	24·3	19·1	42·8	7·4	48·6
	10 min	17·1	12·9	28·6	5·6	35·7
	15 min	12·9	7·0	18·7	4·0	32·2
	30 min	7·8	3·0	10·7	0·8	26·6
	60 min	4·1	1·5	5·9	0·7	16·6
Erosivity gradient (N h^{-1} km^{-1})	Total	2·8	1·3	4·8	0·3	31

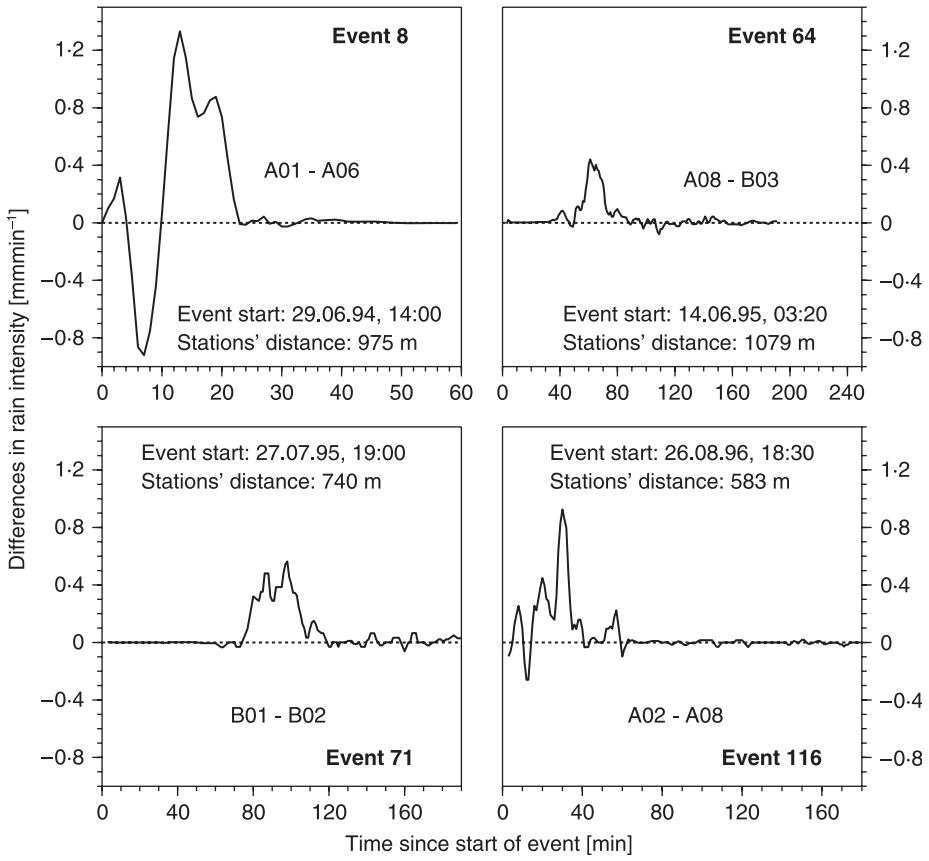

Figure 8. Differences in rain intensity between station pairs represented in Figure 7 for four events; intensities are smoothed using a moving average of 3 min.

(iii) the lack of a minimum or maximum within the research area, and (iv) the short periods during which the main portion of the trend develops indicate that the trend is caused by convective cells, which are larger than the research area (1·4 km^2). The steep gradient of the trend, however, makes it unlikely that they are much larger. These trends are hence likely to be underestimated with most methods commonly applied to determine the spatial variation in rainfall.

Our definition of gradient events selected only rains for which the gradient was detectable for the total rain depth. Our definition did not include those gradient events for which a movement of a high-intensity cell cancelled out the effect and those events for which the trend during short periods of rain was too small to override the random error within the measurements. In both cases, the effects on surface hydrology should be small. Hence our conservative definition, although incomplete, should give an appropriate estimate of the hydrological significance of gradient events.

Influence of climate on spatial trends on a sub-kilometre scale

There are only a few studies focusing on small-scale (<10 km^2) spatial variability in rainfall depth and intensity (e.g. Hernandez *et al*., 2000; Goodrich *et al*., 1995; Niemczynowicz, 1982; Sivakumar and Hatfield, 1990; Jensen and Pedersen, 2005). A study similar to the one presented here was carried out by Goodrich *et al*. (1995) in the 4·4 ha semi-arid experimental watershed part of the Walnut Gulch experimental site in Arizona. Linear trends in rain depth exhibited gradients between 2·8 and 24·8 mm km^{-1} (mean 12 mm km^{-1}) for nine out of 11 events. These gradients were about twice as large as the gradients at the Scheyern test site. Niemczynowicz (1982) evaluated the spatial representativeness of point rain measurements (12 rain gauges, three-year observation) in a 25 km^2 urban watershed in Sweden. The structure of the events was not tested but from his data a maximum gradient

DOI: 10.1002/esp

of 5·5 mm km^{-1} can be derived, which is only one-third of the maximum gradient found at Scheyern (15·7 mm km^{-1}). Thus, the gradients seem to increase from the maritime Swedish situation to the sub-continental Scheyern climate and further to the semi-arid, continental climate in Arizona.

Sub-kilometre scale spatial trends increase with storm size and recurrence interval

Spatial variability of rain depth in a small semi-arid tropical environment was tested by Sivakumar and Hatfield (1990) during two years at 18 rain gauges within a flat 500 ha area. In general, the authors found that spatial variability within the test site increased with storm size. Our study of gradient events shows that also within an event the spatial variability is largest during the high-intensity periods (Table IV). Nevertheless, a trend cannot be generally assumed for any high-intensity period because high intensities were more or less equally distributed between spatial gradient events and random events. For example, $I_{max60} > 10$ mm was measured four times for gradient events but also four times for random events. Hence, the need to set up a dense network of rain gauges increases (i) with decreasing time interval a respective process is looked at, and (ii) with the influence that single, rare storms have on the respective process because the strength of the gradient increased with increasing size of recurrence interval (Table V). Hence, if runoff and erosion scenarios for small watersheds are evaluated the potential effects of spatial trends in rainfall become more and more important if rains with increasing recurrence intervals are assumed.

Process significance of spatial trends on the sub-kilometre scale

During the four-year observation period spatial gradient events did not occur later than early September. There might be few more gradient events during the winter-half year, which we did not evaluate because of measurement induced variability (snow fall, increasing wind speed error) and failures in measuring stations (snow frozen in funnels, frozen tipping buckets) increase in the winter half-year. Also focusing on events ≥ 5 mm only restricted the total number of gradient events. Therefore, our estimated number of gradient events determined during the observation period is conservative. However, the additional events would have only a small impact on most processes due to their small precipitation depth and flat gradients.

Due to the very short period during which the differences develop, the importance of gradient events increases with decreasing temporal scale of a process. While gradient events are almost unimportant for annual processes like groundwater recharge, they are highly important for rain erosivity or runoff. Their importance is even higher where a certain threshold has to be exceeded for a process to occur. Such a threshold process would be rill initiation (e.g. Van Oost *et al*., 2004; Fiener *et al*., 2008). The threshold may be exceeded on one field while the peak intensity remains below the threshold on the neighbouring field. Thus, a large difference in the response of the two fields would result despite a relatively small difference in total rain.

Focusing on surface runoff and soil erosion in small agricultural watersheds the hydrological summer half-year and especially the months June to August are important at the research site, as these time periods receive about 90% and 70% of the annual erosivity, respectively (Schwertmann *et al*., 1987). During the four-year observation period about one-third of all summer events and about half of all events between June and August had a spatial trend. Hence, spatial trends of rain events are significant for small watersheds and should be considered when developing, calibrating, validating and applying event-based runoff and erosion models. Trends in rain intensity and rain erosivity may also contribute to the differences in soil loss observed from replicated plots (e.g. Nearing *et al*., 1999).

Conclusions

A network of 13 rain gauges at a 1·4 km^2 test site in southern Germany exhibited a significant spatial trend in rainfall depth for 33% of all events during the summer half-year. The individual trends were essentially linear. Gradients in rainfall depth ranged from 1·0 to 15·7 mm km^{-1} with a mean of 4·2 mm km^{-1} (median 3·3 mm km^{-1}) and were clearly not due to errors of the measuring systems or wind effects. While the spatially random events produced about 20% more rain than gradient events, the cumulative rain erosivity of the gradient events was about 40% larger. The gradients in rain lead to much steeper gradients in predicted rain erosivity and predicted runoff. Rain depth of gradient rains on average increased within 1 km distance by 48% of the rain at the central location. In contrast this average increase was more than twice as steep for rain erosivity and runoff.

The trends had no significantly preferred orientation. This suggests that in the longer term there is no difference in rainfall depth within the test site, but in short-time periods or for single events the assumption of spatially uniform rainfall is invalid on the sub-kilometre scale. This seems to apply to many regions where summer rainfall is connected to convective storms and has important implications for any kind of small-scale environmental research depending on appropriate rainfall data.

Table V. Breakdown of average rain trends of all erosive events in the hydrological summer-half year (1994–1997) by the recurrence intervals according to Bartels *et al*. (1997); where recurrence intervals differed for the 15-, 30- or 60-min maximum intensity of an event, it is assigned to the minimum recurrence interval

	All events		Gradient events		
Recurrence (yr)	Average gradient (mm km^{-1})	Number of events	Average gradient (mm km^{-1})	Number of events	Number of random events
5–10	10·7	2	10·7	2	0
1–5	3·9	5	9·8	2	3
0·5–1	2·7	16	4·8	9	7
<0·5	0·6	36	2·6	9	27
All	1·8	59	4·9	22	37

DOI: 10.1002/esp

The strength of the spatial trend was not related to rain depth but increased with rain intensity. The trends thus also increased in strength with recurrence interval. Moreover, the gradients of maximum intensities were more pronounced compared to those of rain depth. This has important implications for any hydrological or geomorphologic process sensitive to maximum rain intensities, especially when focusing on large, rare events. As an example shown for rain erosivity, relative gradients of derived environmental parameters can be much steeper than those of rain depth or intensity. Hence, it will take considerably longer until sub-kilometre scale differences in such parameters level out than the time needed to level out difference in rain depth. These farm-scale differences are highly relevant for environmental processes acting on short-time scales like flooding or erosion. They should be considered during establishing, validating and application of any event-based erosion (or hydrological) model.

Acknowledgements—The scientific activities of the research network 'Forschungsverbund Agrarökosysteme München' (FAM) were financially supported by the German Federal Ministry of Education and Research (BMBF 0339370). Overhead costs of the research station of Scheyern were funded by the Bavarian State Ministry for Science, Research and Arts. The continuous technical supervision and maintenance of the stations was carried out by Richard Wenzel and Bernhard Johannes. The help with statistical analyses by Bernhard Johannes, Max Wittmer and Josef Nipper is gratefully acknowledged. The actual research is part of the German Research Agency (DFG) project DI 639/1-1 (Markus Disse).

References

Adami A, Da Deppo L. 1986. *On the Systematic Errors of Tipping Bucket Recording Rain Gauges*. Proceedings of the Correction of Precipitation Measurements. ETH/IAHS/WMO workshop on the correction of precipitation measurements, Zürich; 27–30.

Arora M, Singh P, Goel NK, Singh RD. 2006. Spatial distribution and seasonal variability of rainfall in a mountainous basin in the Himalayan region. *Water Resources Management* **20**: 489–508. DOI: 10.1007/s11269-006-8773-4

Bartels H, Malitz G, Asmus S, Albrecht FM, Dietzer B, Günther T, Ertel H. 1997. *Starkniederschlaghöhen für Deutschland – KOSTRA* [*Recurrence time of rain intensities – KOSTRA*] Deutscher Wetterdienst: Offenbach a. Main (in German).

Bastin G, Lorent B, Duque C, Gevers M. 1984. Optimal estimation of the average areal rainfall and optimal selection of rain-gauge locations. *Water Resources Research* **20**: 463–470.

Berne A, Delrieu G, Creutin JD, Obled C. 2004. Temporal and spatial resolution of rainfall measurements required for urban hydrology. *Journal of Hydrology* **299**: 166–179.

Borga M. 2002. Accuracy of radar rainfall estimates for streamflow simulation. *Journal of Hydrology* **267**: 26–39.

Borga M, Vizzaccaro A. 1997. On the interpolation of hydrologic variables: formal equivalence of multiquadratic surface fitting and kriging. *Journal of Hydrology* **195**: 160–171.

Bronstert A, Bárdossy A. 2003. Uncertainty of runoff modelling at the hillslope scale due to temporal variations of rainfall intensity. *Physics and Chemistry of the Earth* **28**: 283–288.

Buytaert W, Celleri R, Willems P, De Bievre B, Wyseure G. 2006. Spatial and temporal rainfall variability in mountainous areas: a case study from the south Ecuadorian Andes. *Journal of Hydrology* **329**: 413–421.

Datta S, Jones WL, Roy B, Tokay A. 2003. Spatial variability of surface rainfall as observed from TRMM field campaign data. *Journal of Applied Meteorology* **42**: 598–610.

Desa MNM, Niemczynowicz J. 1997. Dynamics of short rainfall storms in a small scale urban area in Coly Limper, Malaysia. *Atmospheric Research* **44**: 293–315.

Diggle PJ, Ribeiro Jr PJ. 2007. *Model-based Geostatistics*. Springer: New York.

Faurès J-M, Goodrich DC, Woolhiser DA, Sorooshian S. 1995. Impact of small-scale spatial rainfall variability on runoff modeling. *Journal of Hydrology* **173**: 309–326.

Fiener P, Auerswald K. 2007. Rotation effects of potato, maize and winter wheat on soil erosion by water. *Soil Science Society of America Journal* **71**: 1919–1925.

Fiener P, Govers G, Van Oost K. 2008. Evaluation of a dynamic multi-class sediment transport model in a catchment under soil-conservation agriculture. *Earth Surface Processes and Landforms* **33**: 1639–1660.

Goodrich DC, Faures JM, Woolhiser DA, Lane LJ, Sorooshian S. 1995. Measurement and analysis of small-scale convective storm rainfall variability. *Journal of Hydrology* **173**: 283–308.

Hernandez M, Miller SN, Goodrich DC, Goff BF, Kepner WG, Edmonds CM, Jones KB. 2000. Modeling runoff response to land cover and rainfall spatial variability in semi-arid watersheds. *Environmental Monitoring and Assessment* **64**: 285–298.

Jensen NE, Pedersen L. 2005. Spatial variability of rainfall: variations within a single radar pixel. *Atmospheric Research* **77**: 269–277.

Johannes B. 2001. *Ausmaß und Ursachen kleinräumiger Nieder-Schlagsvariabilität und Konzequenzen für die Abflussbildung* [*Extend and Cause of Spatial Rain Variability in Small Areas – Effects on Surface Runoff*], FAM-Bericht 50. Shaker: Aachen (in German).

Kirkby MJ, Bracken LJ, Shannon J. 2005. The influence of rainfall distribution and morphological factors on runoff delivery from dryland catchments in SE Spain. *Catena* **62**: 136–156.

Kruizinga S, Yperlaan GJ. 1978. Spatial interpolation of daily totals of rainfall. *Journal of Hydrology* **36**: 65–73.

La Barbera P, Lanza LG, Stagi L. 2002. Tipping bucket mechanical errors and their influence on rainfall statistics and extremes. *Water Science and Technology* **45**: 1–9.

Mockus V. 1972. Estimation of direct runoff from storm rainfall. In *SCS National Engineering Handbook. Section 4. Hydrology*. USDA: Washington, DC.

Molini A, Lanza LG, La Barbera P. 2005. Improving the accuracy of tipping-bucket rain records using disaggregation techniques. *Atmospheric Research* **77**: 203–217.

Nearing MA. 1998. Why soil erosion models over-predict small soil losses and under-predict large soil losses. *Catena* **32**: 15–22.

Nearing MA, Govers G, Norton DL. 1999. Variability in soil erosion data from replicated plots. *Soil Science Society of America Journal* **63**: 1829–1835.

Nielsen DR, Wendroth O. 2003. *Spatial and Temporal Statistics: Sampling Field Soils and their Vegetation*. Catena Verlag: Cremmlingen.

Niemczynowicz J. 1982. Areal intensity–duration–frequency curves for short-term rainfall events in Lund. *Nordic Hydrology* **13**: 193–204.

Nyssen J, Vandenreyken H, Poesen J, Moeyersons J, Deckers J, Haile M, Salles C, Govers G. 2005. Rainfall erosivity and variability in the Northern Ethiopian Highlands. *Journal of Hydrology* **311**: 172–187.

Overgaard S, El-Shaarawi AH, Arnbjerg-Nielsen K. 1998. Calibration of tipping bucket rain gauges. *Water Science and Technology* **37**: 139–145.

Papamichail DM, Metaxa IG. 1996. Geostatistical analysis of spatial variability of rainfall and optimal design of a rain gauge network. *Water Resources Management* **10**: 107–127. DOI: 10.1007/BF00429682

Pebesma EJ. 2004. Multivariable geostatistics in S: the gstat package. *Computers & Geosciences* **30**: 683–691.

Quirmbach M, Schultz GA. 2002. Comparison of rain gauge and radar data as input to an urban rainfall–runoff model. *Water Science and Technology* **45**: 27–33.

R Development Core Team. 2007. R: a language and environment for statistical computing. http://www.R-project.org [Accessed 20 September 2007].

Richter D. 1995. *Ergebnisse methodischer Untersuchungen zur Korrektur des systematischen Meßfehlers des Hellmann-Niederschlagsmessers* [*Analysis of Methods to Correct Systematic Errors of Hellmann Rain Gauges*]. DWD Offenbach Selbstverlag: Offenbach (in German).

Samiuddin M. 1970. On a test for an assigned value of correlation in a bivariate normal distribution. *Biometrika* **57**: 461–464.

Schuurmans JM, Bierkens MFP, Pebesma EJ, Uijlenhoet R. 2007. Automatic prediction of high-resolution daily rainfall fields for multiple extents: the potential of operational radar. *Journal of Hydrometeorology* **8**: 1204–1224.

Schwertmann U, Vogl W, Kainz M. 1987. *Bodenerosion durch Wasser – Vorhersage des Abtrags und Bewertung von Gegenmaßnahmen* [*Soil Erosion by Water – Prediction of Soil Loss and Valuation of Counter-measures*]. Ulmer Verlag: Stuttgart (in German).

Sinowski W, Auerswald K. 1999. Using relief parameters in a discriminant analysis to stratify geological areas with different spatial variability of soil properties. *Geoderma* **89**: 113–128.

Sivakumar MVK, Hatfield JL. 1990. Spatial variability of rainfall at an experimental station in Niger, West Africa. *Theoretical and Applied Climatology* **42**: 33–39. DOI: 10.1007/BF00865524

Stow CD, Dirks KN. 1998. High-resolution studies of rainfall on Norfolk Island: Part 1. The spatial variability of rainfall. *Journal of Hydrology* **208**: 163–186.

Syed KH, Goodrich DC, Myers DE, Sorooshian S. 2003. Spatial characteristics of thunderstorm rainfall fields and their relation to runoff. *Journal of Hydrology* **271**: 1–21.

Taupin JD. 1997. Characterization of rainfall spatial variability at a scale smaller than 1 km in a semiarid area (region of Niamey, Niger). *Comptes Rendus de l Academie des Sciences Serie Ii Fascicule A-Sciences de la Terre et des Planetes* **325**: 251–256.

Tsanis IK, Gad MA, Donaldson NT. 2002. A comparative analysis of rain-gauge and radar techniques for storm kinematics. *Advances in Water Resources* **25**: 305–316.

Van Oost K, Beuselinck L, Hairsine PB, Govers G. 2004. Spatial evaluation of multi-class sediment transport and depositon model. *Earth Surface Processes and Landforms* **29**: 1027–1044.

Voltz M, Webster R. 1990. A comparison of kriging, cubic splines and classification for predicting soil properties from sample information. *Journal of Soil Science* **41**: 473–490.

Webster R, Oliver MA. 2000. *Geostatistics for Environmental Scientists*. John Wiley & Sons: Chichester.

Wischmeier WH, Smith DD. 1960. *A Universal Soil-loss Equation to Guide Conservation Farm Planning*. International Society of Soil Science: Madison, WI.

Wischmeier WH, Smith DD. 1978. *Predicting Rainfall Erosion Losses – A Guide to Conservation Planning*. US Government Print Office: Washington, DC.